Carbohydrate Polymers 95 (2013) 134–142

Contents lists available at SciVerse ScienceDirect

Carbohydrate Polymers

journal homepage: www.elsevier.com/locate/carbpol

Development and characterization of novel alginate-based hydrogels as vehicles for bone substitutes

D.S. Morais[a,1], M.A. Rodrigues[b,1], T.I. Silva[c], M.A. Lopes[b,*], M. Santos[d,e], J.D. Santos[b], C.M. Botelho[a]

[a] Instituto de Biotecnologia e Bioengenharia, Centro de Engenharia Biológica, Universidade do Minho, Campus de Gualtar, 4710-057 Braga, Portugal
[b] CEMUC, Departamento de Engenharia Metalúrgica e Materiais, Faculdade de Engenharia, Universidade do Porto, Rua Dr. Roberto Frias, 4200-465 Porto, Portugal
[c] Departamento de Engenharia Metalúrgica e Materiais, Faculdade de Engenharia, Universidade do Porto, Rua Dr. Roberto Frias, 4200-465 Porto, Portugal
[d] Biosckin, Molecular and Cell Therapies S.A., Rua Engenheiro Frederico Ulrich, 2650 4470-605 Moreira da Maia, Portugal
[e] CECA-ICETA Campus Agrário de Vairão, Rua P. Amando Quintas, 4485-661 Vairão, Portugal

ARTICLE INFO

Article history:
Received 21 November 2012
Received in revised form 17 February 2013
Accepted 27 February 2013
Available online 6 March 2013

Keywords:
Injectable bone substitute
Alginate-based hydrogels
Bone regeneration
Physical–chemical characterization

ABSTRACT

In this work three different hydrogels were developed to associate, as vehicles, with the synthetic bone substitute GR-HAP. One based on an alginate matrix (*Alg*); a second on a mixture of alginate and chitosan (*Alg*/*Ch*); and a third on alginate and hyaluronate (*Alg*/*HA*), using Ca^{2+} ions as cross-linking agents. The hydrogels, as well as the respective injectable bone substitutes (*IBSs*), were fully characterized from the physical–chemical point of view. Weight change studies proved that all hydrogels were able to swell and degrade within 72 h at pH 7.4 and 4.0, being *Alg*/*HA* the hydrogel with the highest degradation rate (80%). Rheology studies demonstrated that all hydrogels are non-Newtonian viscoelastic fluids, and injectability tests showed that *IBSs* presented low maximum extrusion forces, as well as quite stable average forces. In conclusion, the studied hydrogels present the necessary features to be successfully used as vehicles of GR-HAP, particularly the hydrogel *Alg*/*HA*.

1. Introduction

Every year, millions of patients, worldwide, are affected by bone defects caused by bone disorder or injury (Bostrom & Seigerman, 2005; Giannoudis, Dinopoulos, & Tsiridis, 2005; Vaccaro, 2002). In the last years, synthetic bone substitutes, mainly based on hydroxyapatite (HAP) and tricalcium phosphate, have been developed as treatment for those bone defects. These substitutes present several advantages against autografts or xenografts, namely, their unlimited availability and the fact that they eliminate the risk of disease transmission (Giannoudis et al., 2005; Moore, Graves, & Bain, 2001; Zimmermann & Moghaddam, 2011). To improve the chemical similarity between these bioceramics and bone inorganic part, glass-reinforced hydroxyapatite (GR-HAP) composites have been developed (Lopes, Knowles, Santos, Monteiro, & Olsen, 1999; Lopes, Knowles, & Santos, 2000; Salih, Georgiou, Knowles, & Olsen, 2001).

In order to potentiate the clinical application of the synthetic substitutes, they have also been developed in injectable form, by association with hydrogels. This approach presents some advantages, it can decrease the surgery time, allow a better fill of the bone defects and facilitate the substitute application in clinical situations with a difficult access to the defect. The hydrogel, working as a vehicle, should present a suitable viscosity to enable the bone substitute granules injectability (Couto, Hong, & Mano, 2009; Gaharwar, Dammu, Canter, Wu, & Schmidt, 2011; Larsson & Hannink, 2011; Liu et al., 2006; Oliveira et al., 2010).

Alginate is a polysaccharide produced mainly from brown seaweeds. It is a linear binary co-polymer composed of (1-4)-linked β-D-mannuronic acid (M) and α-L-guluronic acid (G) residues as monomers, constituting M-, G-, and MG-sequential block structures (Nunamaker, Purcell, & Kipke, 2007; Pawar & Edgar, 2012; Stevens, Qanadilo, Langer, & Prasad Shastri, 2004). This polymer has been widely used to produce biomedical hydrogels, mainly due to its biocompatibility, biodegradation, gel-forming ability through simple divalent cations (such as Ca^{2+}, Ba^{2+} and Sr^{2+}) addition and its very low cost (Lee & Mooney, 2011; Ueng et al., 2004; Ulery, Nair, & Laurencin, 2011). For pH values above alginate pK_a value (about 3.38 and 3.65 for M and G residues, respectively) it presents a polyanionic chemical structure, the monomers carboxylic groups are negatively charged (Andersen, Strand, Formo, Alsberg, & Christensen, 2012; Funami et al., 2009). Thus, the cations bind to them, preferentially toward the G-block rather than the

* Corresponding author. Tel.: +351 936251083.
E-mail address: malopes@fe.up.pt (M.A. Lopes).
[1] Both authors contributed equally to this work.

0144-8617/$ – see front matter © 2013 Elsevier Ltd. All rights reserved.
http://dx.doi.org/10.1016/j.carbpol.2013.02.067

M-block, forming a structure named as "egg-box" and providing the cross-linking of the polymeric chains (Davidovich-Pinhas & Bianco-Peled, 2010; Nunamaker et al., 2007; Pawar & Edgar, 2012). When G monomer proportion is higher than M monomer proportion, a strong brittle gel will be obtained. When M proportion is higher, the hydrogel will be weaker, but more flexible, because there are less junction zones between chains (Nunamaker et al., 2007; Pawar & Edgar, 2012; Sriamornsak, Thirawong, & Korkerd, 2007). Alginate hydrogels have already been used in bone tissue engineering as vehicles of HAP, allowing to properly fill the whole bone defect. To produce biomedical alginate hydrogels, Ca^{2+} ions are the most used crosslinking agents due to the mild reaction conditions compared to the cellular toxicity of both Ba^{2+} and Sr^{2+}. Moreover, for bone application this ion is preferred since it is the main extracellular matrix (ECM) ion. However, in biomedical applications, alginates have the main disadvantage of being non-biologically active, presenting a low cell adhesion (Andersen et al., 2012; Nair & Laurencin, 2007; Nunamaker et al., 2007; Ulery et al., 2011).

One way of improving the biological properties of alginate scaffolds, it is to ionically associate it to another polymer, namely a polycation as chitosan, forming a polyelectrolyte complex (Chen et al., 2009; Chunga et al., 2001). Thus, a complex between alginate and another polyanion, such as hyaluronic acid (HA), can also be formed using cations as intermediate agents (Oerther et al., 2000). Obviously, to ensure the complexes formation, the solution pH has to be controlled for the two polymers being charged (Dakhara & Anajwala, 2010).

In the present study, we developed three different alginate-based hydrogels for being used as vehicles of the GR-HAP bone substitute granules. One hydrogel was just composed by alginate cross-linked with Ca^{2+} ions, and other two hydrogels resulted from the association of chitosan and hyaluronic acid to alginate. The developed hydrogels were submitted to a physical–chemical characterization, as well as the respective injectable systems composed by each hydrogel and the GR-HAP granules.

2. Materials and methods

2.1. Materials

Alginic acid sodium salt from brown algae (bioreagent grade; low viscosity; 39% (w/w) of guluronic acid and 61% (w/w) of mannuronic acid), hyaluronic acid sodium salt from *Streptococcus equi* and calcium chloride hexahydrate ($CaCl_2{\cdot}6H_2O$, medical grade) were purchased from *Sigma* (USA). Chitosan HCl (medical grade) was purchased from *Heppe Medical Chitosan GmbH* (Germany). The hydroxyapatite powder was purchased from *Plasma Biotal* (UK).

2.2. Methods

2.2.1. Hydrogels preparation

2.2.1.1. Hydrogel Alg. Sodium alginate was dissolved overnight in deionized water at room temperature, in order to prepare a polymeric solution with a concentration of 7% (w/V) with pH 6. $CaCl_2{\cdot}6H_2O$ was also dissolved in deionized water to a concentration of 15 mg/mL. Finally, the $CaCl_2$ solution was added to the sodium alginate solution at a proportion of 1:4 (V_{CaCl_2} : $V_{\text{sodium alginate}}$).

2.2.1.2. Hydrogel Alg/Ch. Chitosan HCl was dissolved in deionized water to prepare a solution of 0.5% (w/V). Then, the $CaCl_2$ and sodium alginate solution were added to it, by this order, in the proportions of 1:4 (V_{CaCl_2} : $V_{\text{sodium alginate}}$) and 1:1 ($V_{\text{sodium alginate}}$: $V_{\text{chitosan HCl}}$), respectively.

2.2.1.3. Hydrogel Alg/HA. Sodium hyaluronate was dissolved overnight in deionized water, at 4 °C, to a concentration of 0.5% (w/V). This solution was added to the sodium alginate solution in a proportion of 1:1 ($V_{\text{sodium alginate}}$: $V_{\text{sodium hyaluronate}}$). Finally, to the solution of the two polymers the $CaCl_2$ solution was added in a proportion of 1:4 (V_{CaCl_2} : $V_{\text{sodium alginate}}$).

2.2.2. GR-HAP and injectable bone substitutes (IBSs) preparation

2.2.2.1. GR-HAP. GR-HAP was obtained by adding 2.5% (w/w) of glass (with the composition $65P_2O_5$–$15CaO$–$10CaF_2$–$10Na_2O$, mol%) to pure phase of prepared HAP mixed with microcrystalline cellulose. Then, discs were prepared by uniaxial pressing and heat treated at 600 °C to burn out the microcrystalline cellulose and then sintered at 1300 °C for 1 h. Finally the discs were milled and sieved to produce granules of a 500–1000 μm size range.

2.2.2.2. IBSs. In order to optimize the preparation of the three different *IBS*s, GR-HAP granules were simply mixed and aggregated with each one of the developed hydrogels until the desired consistency was achieved. For each system, the used apparent ideal proportions (w/w) of the bone substitute and each hydrogel were, respectively: *Alg_IBS* – 41% of hydrogel and 59% of GR-HAP; *Alg/Ch_IBS* – 47% of hydrogel and 53% of GR-HAP; *Alg/HA_IBS* – 48% of hydrogel and 52% of GR-HAP.

2.2.3. Scanning electron microscopy (SEM) analysis

On the case of the *IBS*s, the samples were firstly fixed with 1.5% (w/V) glutaraldehyde in 0.14 M sodium cacodylate buffer (pH 7.3). Afterwards, the samples were dehydrated using graded ethanol solutions from 50% (V/V) to 100% (V/V), followed by immersion in hexamethyldisilazanes (HMDS) solutions ranging from 50% (V/V) to 100% (V/V). The samples lasted 10 min in each ethanol and HMDS solution and overnight in 100% (V/V) HMDS. All the used reagents were purchased from *Sigma* (USA). Afterwards, the hydrogels and *IBS*s samples were mounted onto an aluminum stub and coated with gold/palladium using a *SPI Sputter Coater*. Finally, the samples morphology was analyzed using the equipment *FEI Quanta 400FEG SEM* (*FEI*, USA).

2.2.4. Fourier transform infrared – attenuated total reflectance (FTIR-ATR) spectroscopy analysis

The FTIR-ATR spectra, over the wavelength range of 1800–800 cm^{-1}, of the sodium alginate, chitosan HCl and sodium hyaluronate polymeric solutions, and of the three developed hydrogels were obtained by the FTIR spectrometer *FT/IR-4100* (*Jasco*, USA). FTIR-ATR analysis of the sodium alginate powder before and after autoclaving was also performed over the wavelength range of 2000–750 cm^{-1}.

2.2.5. Hydrogels swelling profile

Swelling studies were performed according to ASTM (American Society for Testing and Materials) F2900-11. For that, the hydrogels were immersed (in quadriplicate) in two different buffer solutions, phosphate buffered saline (PBS: pH 7.4, *Sigma*, USA) and potassium hydrogen phthalate (KHP: pH 4.0, *Sigma*, USA) as follows.

A sample of each gel was weighed before immersion in any of the solutions and it was designated as W_0. Afterwards, the samples were placed inside a previously weighed standard mesh and immersed in the buffers and incubated at 37 °C. The mesh was removed every minute for 5 min and left to dry until no drop was formed. The gel/mesh system was weighed and the mesh weight was subtracted to the system weight and designated as W_t. The weight change (%) for each sample at time t, was calculated using the following equation: $\textit{Weight change}\ (\%) = (W_t - W_0)/W_0 \times 100$.

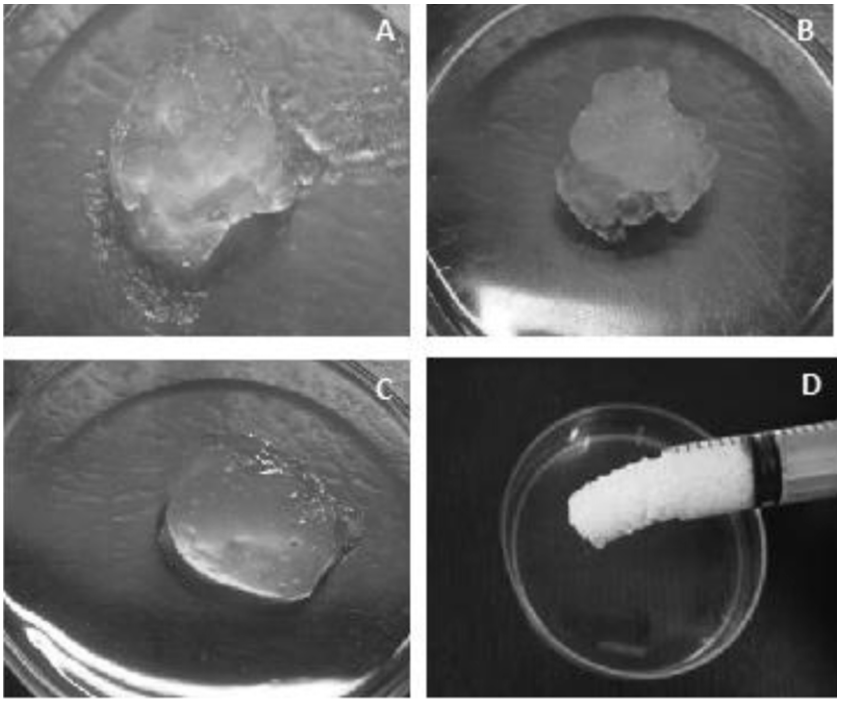

Fig. 1. Macroscopic appearance of the three developed hydrogels: (A) *Alg* hydrogel; (B) *Alg*/*Ch* hydrogel; (C) *Alg*/*HA* hydrogel; (D) macroscopic appearance of the *Alg*_*IBS*.

2.2.6. Hydrogels degradation profile

Hydrogels degradation studies were performed according to ASTM F2900-11, using two different buffer solutions, PBS (pH 7.4) and KHP (pH 4.0) as follows.

Firstly, *IBS*s were prepared (in triplicate) according to Section 2.2.2.2. Both GR-HAP and hydrogels weights were recorded, and the hydrogel weight was designated as W_0. All samples were enclosed in glass vessels with each of the above-mentioned buffer solution and incubated at 37 °C and 1 Hz orbital agitation. *IBS*s were removed at 24 and 72 h, carefully filtered and weighed. After subtracting GR-HAP's weight, this final weight was designated as W_t. The degradation percentage was calculated using the following equation: $Degradation\ (\%) = (W_0 - W_t)/W_0 \times 100$.

2.2.7. Rheology tests

The rheological behavior of the three hydrogels was evaluated by performing measurements with the rheometer *Physica MCR-300* (*Anton Paar*, Austria), employing the concentric cylinders geometry. To perform the flow measurements of each hydrogel, 1 mL of the material was introduced between the cylinders, and this procedure was done in duplicate. The measurements were performed at 20 °C, between 1 and 100 s^{-1} frequencies.

2.2.8. Injectability tests

To evaluate the injectability of the three developed *IBS*s, equal volume of each one was placed in a 2 mL syringe, which was fixed vertically on the texture analyzer *TA-XT2i* (*Stable Mycro Systems*, UK). During the test, while using a load cell of 5 kgf, the syringe piston was pushed at a velocity of 1 mm/s, through a distance of 10 mm. For each *IBS* the test was performed in triplicate.

2.2.9. Statistical analysis

Experimental data was presented as mean ± SD (standard deviation). Statistical analysis of data was performed using the one-way ANOVA and the Bonferroni post hoc analysis, with the software *SigmaStat* 3.5. The differences were considered to be significant at a level of $p < 0.05$.

3. Results and discussion

3.1. Hydrogels and IBSs macroscopic evaluation

Initially, to produce and optimize the hydrogel *Alg* according to the required handling features of a vehicle for the bone substitute, different sodium alginate and $CaCl_2$ concentrations were tested and the final result evaluated. It was observed that for a given alginate concentration, as the added volume of $CaCl_2$ solution increases the hydrogel becomes stiffer. This fact is caused by a stronger cross-linking due to the higher Ca^{2+} concentration, which leads to more junction zones between chains (Nunamaker et al., 2007; Pawar & Edgar, 2012). Hence, it was considered that the alginate optimal concentration was of 7% (m/V) and cross-linker optimal proportion of 1:4 ($V_{CaCl_2} : V_{sodium\ alginate}$).

As observed in Fig. 1, the three developed hydrogels present distinct aspects. Visually, hydrogels *Alg* and *Alg*/*HA* have a homogeneous aspect (Fig. 1A and C), while the hydrogel *Alg*/*Ch* has a heterogeneous aspect. It is also important to mention that hydrogel *Alg*/*HA* appears to be more fluid than the other ones.

The three different *IBS*s present similar aspect and handling; the three hydrogels can envelop and aggregate the GR-HAP granules well, maintaining a whole and moldable structure, as observed in Fig. 1D. These characteristics are extremely important as they allow a simple and efficient application of the material by simply injecting the bone substitute into the bone defect. However, it should be referred that hydrogel *Alg* maintains the injectable (GR-HAP granules plus hydrogel) structure slightly better as a whole, during the injection, without breaking it, which sometimes occurs with the others gels.

3.2. SEM analysis

The *IBS*s morphology was also analyzed by SEM and it is presented in Fig. 2. It is observed, in Fig. 2A1, B1, and C1, that the three hydrogels can involve and aggregate the GR-HAP granules very well. In greater detail, it is possible to observe, in Fig. 2A2,

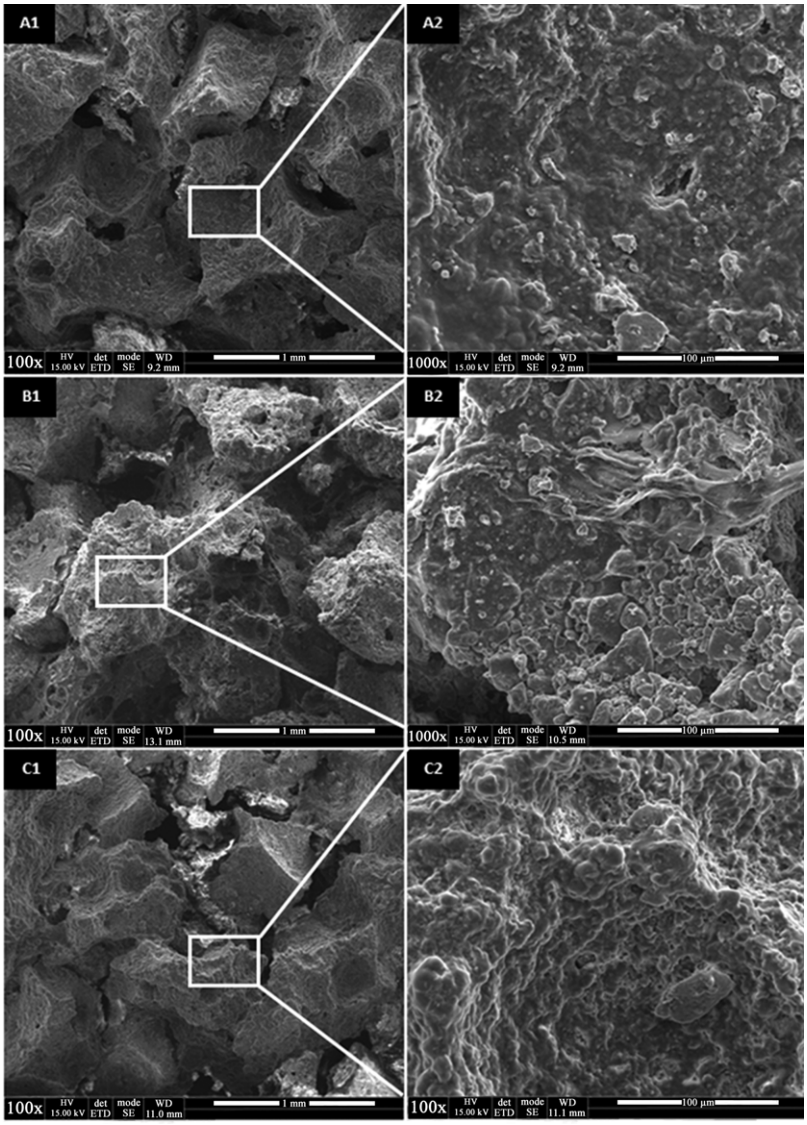

Fig. 2. SEM images of the three injectable systems: (A1 and A2) *Alg_IBS*; (B1 and B2) *Alg/Ch_IBS*; (C1 and C2) *Alg/HA_IBS*.

B2, and C2, polymeric material at the granules surface enveloping them.

3.3. FTIR-ATR spectroscopy analysis

Fig. 3 shows the FTIR-ATR spectra of hydrogels *Alg*, *Alg/Ch*, and *Alg/HA*, and each of the three polymeric solutions used in their preparation. In the spectra region between 1700 cm^{-1} and 1500 cm^{-1}, it is possible to observe a broad band with a peak at 1634 cm^{-1} in all solutions which represents a transmittance band typical of water O—H stretching vibration (Matrajt et al., 2003). This band was expected since water is the major component (>90%, w/V) of all studied solutions. This band cloaks the band expected for the asymmetric stretching vibration of C=O of carboxylic acids (Lasagabaster, Abad, Barral, & Ares, 2006).

At the three polymeric solutions and the hydrogel *Alg* it is possible to observe the typical transmittance bands exhibited by polysaccharides with peaks at 1410 cm^{-1} (assigned to the stretching vibration of C—OH of carboxylic group) and 1034 cm^{-1} (assigned to the stretching vibration of C—O of the alcohol groups) (Papageorgiou et al., 2010). Since no shifts were observed in any of the mentioned spectra, a conclusion can be drawn: the transmittance peaks obtained in the first four spectra, are all due to the presence of alginate. This finding is supported by the total absence of such peaks where alginate is not present (chitosan HCl and sodium hyaluronate solution) and by the decreasing intensity of said peaks in the same proportion as the decreasing concentration of alginate in the hydrogels (Table 1), when compared to the sodium alginate solution concentration. Moreover, it should be referred that the last two spectra showed no fingerprinting regions, because the solutions were of only 0.5% (w/V) of polymer, not being detectable by FTIR analysis (Papageorgiou et al., 2010; Singh et al., 2009).

Table 1
Peaks intensity reduction in hydrogels, when compared to sodium alginate solution.

Hydrogel	Peak (cm^{-1})	Intensity reduction (%)
Alg		42
Alg/Ch	1034	76
Alg/HA		76
Alg		26
Alg/Ch	1410	83
Alg/HA		81

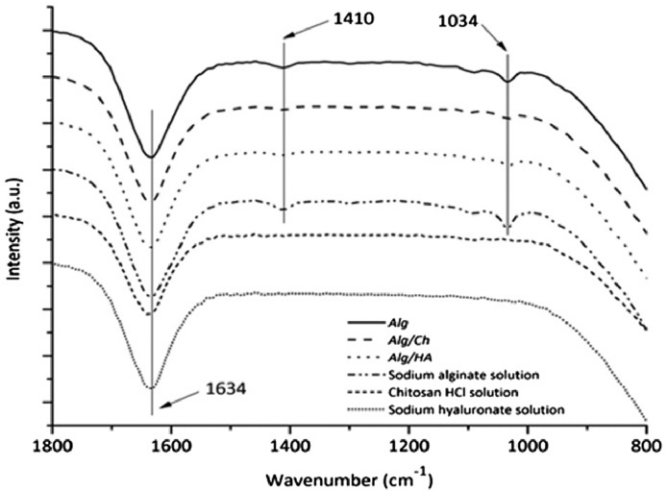

Fig. 3. FTIR-ATR spectra of the three developed hydrogels and the polymeric solutions used to produce them.

3.4. Hydrogels swelling profile

The hydrogels weight change behavior is illustrated in Fig. 4. This study was done using two buffer solutions in order to mimic the pH found at physiological and inflammatory conditions, pH 7.4 and 4.0, respectively. As observed, at the first minute, the three hydrogels undergo a weight increase, for both pH values, due to the swelling phenomenon. This behavior was expected, since by definition hydrogels are able to swell in aqueous solutions (Fedorovich et al., 2007; Gaharwar et al., 2011; Hoffman, 2002). Initially, the osmotic pressure is greater than the forces of the crosslinking bonds that maintain the structure of the polymeric network stable, leading to hydrogel water uptake (Chan & Neufeld, 2009; Davidovich-Pinhas & Bianco-Peled, 2010; Pasparakis & Bouropoulos, 2006). The void regions of the polymer network are filled until an equilibrium state with aqueous medium is reached, increasing the hydrogel volume (Davidovich-Pinhas & Bianco-Peled, 2010; Hoffman, 2002; Slaughter, Khurshid, Fisher, Khademhosseini, & Peppas, 2009). After that time point, the hydrogels *Alg* and *Alg*/*Ch* experience a weight loss, as well as the hydrogel *Alg*/*HA* after 3 min and onward.

It is noticeable that regardless the pH, the weight change behavior of each hydrogel is similar (Fig. 4A and B). Both solutions pH are above alginate pKa, being the carboxylic groups, in both cases, in a charged state, so the cross-linked alginate structure is maintained. Therefore, since the alginate matrix is the base of the three hydrogels there is no change of the hydrogels structure for each pH value, leading to a similar swelling behavior (Andersen et al., 2012; Funami et al., 2009).

When comparing the weight change behavior of each hydrogel, it is visible that the hydrogel *Alg* has a higher swelling ratio than hydrogels *Alg*/*Ch* and *Alg*/*HA*. This difference comes from the polymer concentration difference between hydrogels (Chan & Neufeld, 2009). The higher the polymer concentration within a hydrogel, the lower the water present is, therefore, the osmotic pressure is greater from the medium into the hydrogel (Chan & Neufeld, 2009; Davidovich-Pinhas & Bianco-Peled, 2010). Since the hydrogel *Alg* has lower water content than hydrogels *Alg*/*Ch* and *Alg*/*HA*, the water uptake will be higher, resulting in a larger weight change, as seen in Fig. 4 (Pasparakis & Bouropoulos, 2006).

3.5. Hydrogels degradation profile

These studies were performed due to the vital importance of knowing the degradation profile of any biodegradable biomaterial

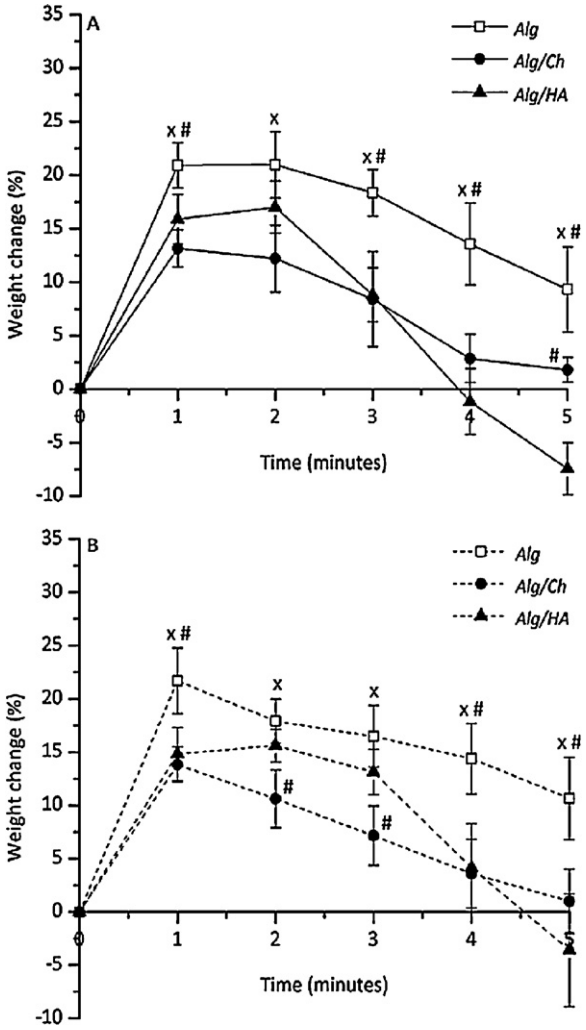

Fig. 4. Weight change of the three hydrogels at 37 °C: (A) PBS (pH 7.4); (B) KHP (pH 4). Data are presented as mean ± SD. $^{x}p < 0.05$-significant difference compared with *Alg*/*Ch*. $^{\#}p < 0.05$-significant difference compared with *Alg*/*HA*.

intended to be implanted. Moreover, for these specific hydrogels application it was defined, as requirement, a 72 h degradation time, being essential to assess this parameter. The tests were performed using the same buffer solutions of swelling tests.

For pH 7.4, Fig. 5A, a degradation percentage increase is observed, for all hydrogels. Hydrogel *Alg* is only composed of cross-linked alginate, and its degradation mechanism is reported as being a result of the glycosidic bonds hydrolysis and the Na^+ ions (present in PBS) interchange with cross-linking Ca^{2+} ions, leading to a weight decrease in time (Dashevsky, 1998; Lee & Mooney, 2011; Lertsutthiwong, Rojsitthisak, & Nimmannit, 2009; Nair & Laurencin, 2007).

Chitosan and HA are also degradable by hydrolysis of the glycosidic bonds (Il'ina & Varlamov, 2004; Kim et al., 2007). Thus, the weight loss of the hydrogels *Alg*/*Ch* and *Alg*/*HA* happens by the hydrolysis of the two constituent polymers of each one and also by the Na^+ ions interchange with Ca^{2+} ions in the alginate matrix. Thereby, the higher degradation of the hydrogels *Alg*/*Ch* and *Alg*/*HA* compared to *Alg*, can be mainly explained by their lower polymeric concentration. In case of the hydrogel *Alg*/*Ch*, there is another possible degradation cause. For a pH 7.4, which is above the chitosan pK_a (6.2–7 range), its amino groups are protonated (Badawy & Rabea, 2011). Therefore, the possible ionic bonds between alginate

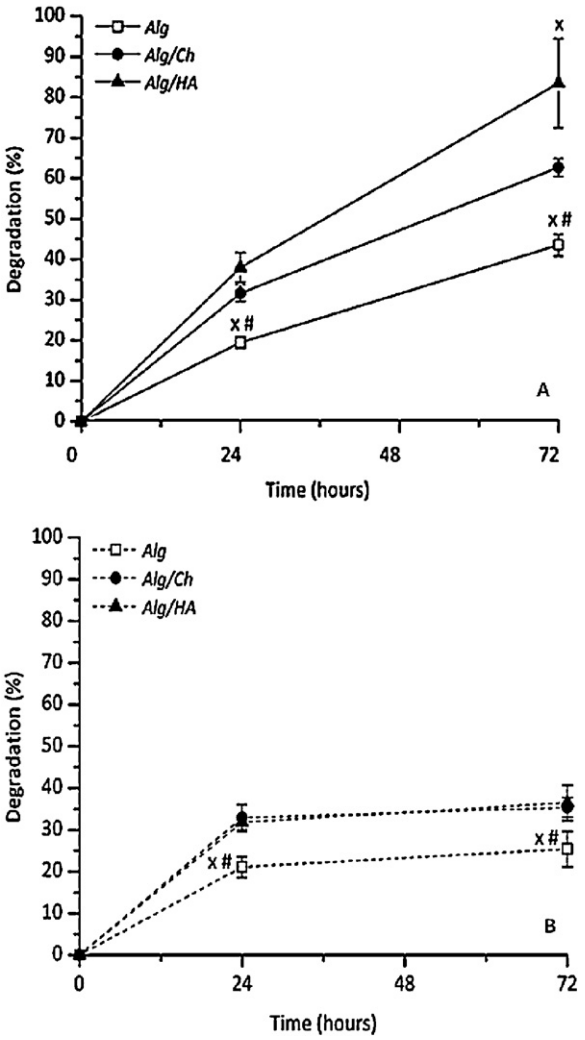

Fig. 5. Degradation of the three hydrogels at 37 °C and 1 Hz orbital agitation: (A) PBS (pH 7.4); (B) KHP (pH 4). Data are presented as mean ± SD. $^{x}p < 0.05$-significant difference compared with *Alg*/*Ch*. $^{\#}p < 0.05$-significant difference compared with *Alg*/*HA*.

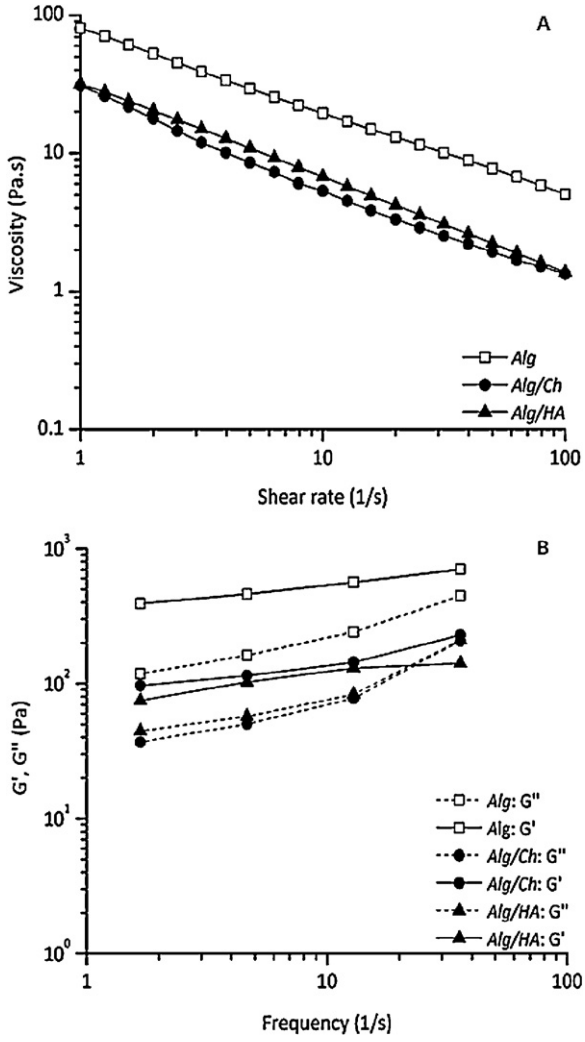

Fig. 6. Rheological characterization of the three developed hydrogels: (A) viscosity frequency dependence; (B) storage modulus (G') and loss modulus (G'') frequency dependence.

carboxylate and chitosan amino groups are broken, improving weight loss (Lertsutthiwong et al., 2009; Li et al., 2010).

The degradation by Na^+ ions interchange with Ca^{2+} ions is more pronounced for a longer exposure time to the medium with Na^+ ions (LeRoux, Guilak, & Setton, 1999). As observed in Fig. 5A, the degradation difference between the hydrogel *Alg*/*HA* and *Alg* or *Alg*/*Ch* is greater at 72 h than at 24 h. This phenomenon can be explained by the fact of the hydrogel *Alg*/*HA* polymeric matrix being supported by ionic interaction between hyaluronate and alginate, mediated by Ca^{2+} ions. Thus, the ions interchange phenomenon has a higher effect in this hydrogel, promoting a higher degradation at 72 h (Oerther et al., 2000).

For pH 4, Fig. 5B, the hydrogels degradation can only happen by hydrolysis of the three polymers, because there are no Na^+ ions and the solution pH is below the chitosan pK_a. Thus, lower degradation values are expected for the three hydrogels at the two time points. In this pH condition, a higher degradation of the hydrogels *Alg*/*Ch* and *Alg*/*HA*, compared to the hydrogel *Alg*, is also verified due to the lower polymeric content. Moreover, as observed in Fig. 5B, for the three hydrogels, the difference between the degradation values at 24 and 72 h is lower than in pH 7.4 solution. This result proves the higher Na^+ ions effect for longer time periods.

3.6. Rheology tests

Since the developed hydrogels are intended to be used in injectable systems it is important to study their rheological features. The rheological characterization of a material involves studies in flow and oscillatory modes (Pelletier et al., 2000; Vallée et al., 2009).

In flow mode, the material viscosity change with the shear rate is evaluated (Pelletier et al., 2000; Vallée et al., 2009). As presented in Fig. 6A, the three hydrogels have a non-Newtonian behavior, because the non-linear relation between the shear rate and the shear stress results in a shear rate dependent of the viscosity, called apparent viscosity (Partal & Franco, 2007; Tadros, 2010). More specifically, the materials have a shear-thinning behavior (pseudoplastic material), meaning that viscosity decreases with shear rate increase (Oerther et al., 2000; Oliveira et al., 2010; Partal & Franco, 2007; Tadros, 2010). This viscosity decrease can be explained by the structural change of the hydrogel polymeric network, due to the shear between the chains. With the velocity gradient increase, the chaotic organization of the hydrogels polymeric chains is converted into an alignment between them according to the flow direction,

leading to a viscosity decrease (Cui, Gupta, & Cummings, 1996; Yucel, Cebe, & Kaplan, 2009).

Additionally, as observed in Fig. 6A, for all shear rate values the hydrogel *Alg* presents a higher viscosity than the other two hydrogels, which have similar viscosity values. The polymeric concentration in the hydrogel, and, the average molecular weight of its constituent polymers are two parameters that determine its viscosity (Oerther et al., 2000; Pelletier et al., 2000). For a higher concentration, maintaining the molecular weight, a higher viscosity is verified. This phenomenon is owed to the polymer chains become closer, promoting the setting of intermolecular associations, leading to the formation of a more compact network. Maintaining the concentration, a higher molecular weight leads to a higher viscosity (Oerther et al., 2000; Pelletier et al., 2000).

The two distinct constituent polymers in the hydrogels *Alg*/*Ch* and *Alg*/*HA* present very different molecular weights, chitosan HCl has a very lower molecular weight than HA, and their polymer concentrations are the same in each hydrogel. However, they present very similar values for every shear rate values. This phenomenon indicates that these hydrogels viscosity is mainly influenced by the alginate concentration in each hydrogel, which is the same. Moreover, the fact of the hydrogel *Alg*, which has a greater alginate concentration than those two, having higher viscosity values is in accordance with this hypothesis (Gargiulo et al., 2010; Manojlovic, Djonlagic, Obradovic, Nedovic, & Bugarski, 2006; Pelletier et al., 2000).

In the oscillatory mode, two parameters can be determined: the storage modulus (G') that quantifies the stored energy, representing the elastic response of the material; the loss modulus (G''), that quantifies the dissipated energy as heat during the process, representing the viscous response of the material (Pelletier et al., 2000; Tadros, 2010). When a material exhibits simultaneously typical behaviors of a viscous liquid and an elastic solid it is named as viscoelastic (Partal & Franco, 2007; Tadros, 2010).

In Fig. 6B, for the three hydrogels, it is showed the G' and G'' values increase with the frequency increase. For all the studied frequencies, the hydrogel *Alg* presents $G' > G''$, indicating a mainly elastic behavior. This was also observed for the other two hydrogels until frequencies of approximately 10 s^{-1}. At the higher studied frequencies, in hydrogel *Alg*/*Ch* and *Alg*/*HA*, an intersection point (*crossover point*) between G' and G'' can be observed. Posteriorly, G'' becomes higher than G' indicating that the materials behavior become more viscous than elastic, revealing that the material structure starts to breakdown (Mason, Dhople, & Wirtz, 1998; Tadros, 2010; Vallée et al., 2009). Once again, the existence of the *crossover point* only in *Alg*/*Ch* and *Alg*/*HA*, can be explained by the lower polymeric concentration relatively to the hydrogel *Alg* (Mason et al., 1998).

Moreover, as depicted in Fig. 6B, for all frequencies, the G'' value of the hydrogel *Alg* is above the other hydrogels G'' values, which are very similar among them. This fact can be related with their viscosity differences discussed previously, namely, the higher viscosity of hydrogel *Alg* may causes the observed higher G'' value (Mason et al., 1998; Pelletier et al., 2000). Moreover, once that G' and G'' can be related by the equation $tan(\delta) = G''/G'$, for the same δ (phase angle shift between sine waves of stress and strain) a material with a higher G'' value has a higher G' value than the other ones, as in Fig. 6B (Mason et al., 1998; Pelletier et al., 2000; Tadros, 2010).

3.7. Injectability tests

In an injectable system it is essential to study the necessary extrusion force to inject the material. In Fig. 7, the injectability curves of the three developed *IBS*s can be observed, they depict

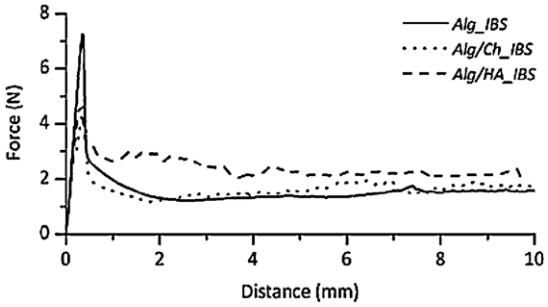

Fig. 7. Injectability curves of the three *IBS*s, at an extrusion velocity of 1 mm/s.

the evolution of the applied force during the material movement through the syringe. In the beginning of the extrusion, maximum forces are observed for the three *IBS*s, being very low: *Alg_IBS* – 7.33 ± 0.19 N; *Alg*/*Ch_IBS* – 4.64 ± 0.32 N ($p < 0.05$ – significant difference compared with *Alg_IBS*); *Alg*/*HA_IBS* – 4.55 ± 0.42 N ($p < 0.05$ – significant difference compared with *Alg_IBS*). Afterwards, the extrusion force decreases, for the three *IBS*s, reaching even lower values and stabilizing during the rest of the injection process, as desired.

During the extrusion process, a very thin hydrogel film is formed between the *IBS*s and the syringe wall. Thus, the higher maximum extrusion force recorded for *Alg_IBS* may be due to a higher static frictional force between the injectable and the syringe wall. Thus, it is necessary to apply a higher extrusion force, in the beginning, in order to initiate the material movement. The other two hydrogels present a lower maximum force, probably, due to a lower static frictional force, so the needed initial extrusion force is lower (Dobre & Ramtal, 2011; Kirkpatrick & Francis, 2007). The higher static frictional force can be explained by the higher viscosity of *Alg*, meaning an increased internal resistance to flow or shear. The viscosity of a fluid can be termed as a drag force and is a measure of the frictional fluid properties, simply put, the less viscous the fluid is, the greater its ease of movement (Dobre & Ramtal, 2011; Murakamia, Sawaea, Horimotob, & Nodac, 1999; Viswanath, Ghosh, Prasad, Dutt, & Rani, 2007).

Usually, between two surfaces, the dynamic frictional force is lower than the static frictional force, which means that to maintain the movement it is necessary a lower force than to start it, as happens in Fig. 7 at about 0.5 mm (Dobre & Ramtal, 2011; Kirkpatrick & Francis, 2007). Afterwards, the dynamic frictional force tends to stabilize in the three gels until the conclusion of the assay, being the medium force similar between them. However, hydrogel *Alg* is the one that presents less force variations, possibly due to previous macroscopically observation that hydrogel *Alg* can aggregate GR-HAP granules slightly better, allowing a more continuous and uniform extrusion.

4. Conclusions

The developed materials presented a characteristic swelling behavior of any hydrogel. It was verified that the hydrogels degradation is mainly due to hydrolysis of the glycosidic bonds and by Na^+ ions interchange with Ca^{2+}. For pH 7.4 the hydrogel *Alg*/*HA* presented the highest degradation, about 80% of weight loss, after 3 days.

A shear-thinning and viscoelastic behavior was verified for the three hydrogels, being the viscosity, G' and G'' mainly influenced by the polymeric content in each hydrogel. The *IBS*s presented low but different maximum extrusion forces, due to the viscosity of the respective polymeric vehicle.

According to the results, the three developed hydrogels are potential vehicles to associate with GR-HAP granules, being able

of well aggregate them, maintaining the injectable system entirety and allowing a good handling of the *IBS* with low and stable injectability forces.

In future, a biological follow-up study must be conducted to ascertain the biomedical application of the developed *IBSs*.

Acknowledgements

The authors would like to acknowledge the financial support from FCT (Fundação para a Ciência e a Tecnologia) through the grant SFRH/BD/76237/2011 and project ENMED/0002/2010, and from FEDER funds through the program COMPETE – Programa Operacional Factores de Competitividade–under the project PEst-C/EME/UI0285/2011, as well as to the project I&DT BIOMAT&CELL no. 1372.

References

Andersen, T., Strand, B. L., Formo, K., Alsberg, E., & Christensen, B. E. (2012). Alginates as biomaterials in tissue engineering. *Carbohydrate Chemistry*, *37*, 227–258.

Badawy, M. E. I., & Rabea, E. I. (2011). A biopolymer chitosan and its derivatives as promising antimicrobial agents against plant pathogens and their applications in crop protection. *International Journal of Carbohydrate Chemistry*, 1–29.

Bostrom, M. P. G., & Seigerman, D. A. (2005). The clinical use of allografts, demineralized bone matrices, synthetic bone graft substitutes and osteoinductive growth factors: A survey study. *HSS Journal*, *1*, 9–18.

Chan, A. W., & Neufeld, R. J. (2009). Modeling the controllable pH-responsive swelling and pore size of networked alginate based biomaterials. *Biomaterials*, *30*, 6119–6129.

Chen, A., Haddad, D., & Wang, R. (2009). Analysis of chitosan–alginate bone scaffolds. *Rutgers University, New Jersey Governor's School of Engineering & Technology*, 1–8.

Chunga, T. W., Yangb, J., Akaikeb, T., Choc, K. Y., Nahd, J. W., Kima, S. I., et al. (2001). Preparation of alginate/galactosylated chitosan scaffold. *Biomaterials*, *23*, 2827–2834.

Couto, D., Hong, Z., & Mano, J. (2009). Development of bioactive and biodegradable chitosan-based injectable systems containing bioactive glass nanoparticles. *Acta Biomaterialia*, *5*, 115–123.

Cui, S. T., Gupta, S. A., & Cummings, P. T. (1996). Molecular dynamics simulations of the rheology of normal decane, hexadecane, and tetracosane. *Journal of Chemical Physics*, *105*, 1214–1220.

Dakhara, S. L., & Anajwala, C. C. (2010). Polyelectrolyte complex: A pharmaceutical review. *Systematic Reviews in Pharmacy*, *1*, 121–127.

Dashevsky, A. (1998). Protein loss by the microencapsulation of an enzyme (lactase) in alginate beads. *International Journal of Pharmaceutics*, *161*, 1–5.

Davidovich-Pinhas, M., & Bianco-Peled, H. (2010). A quantitative analysis of alginate swelling. *Carbohydrate Polymers*, *79*, 1020–1027.

Dobre, A., & Ramtal, D. (Eds.). (2011). *The essential guide to: Physics for flash games, animation, and simulations*. USA: Apress.

Fedorovich, N. E., Alblas, J., Wijn, J. R., Hennink, W. E., Verbout, A. J., & Dhert, W. J. A. (2007). Hydrogels as extracellular matrices for skeletal tissue engineering: State-of-the-art and novel application in organ printing. *Tissue Engineering*, *13*, 1905–1925.

Funami, T., Fang, Y., Noda, S., Ishihara, S., Nakauma, M., Draget, K. I., et al. (2009). Rheological properties of sodium alginate in an aqueous system during gelation in relation to supermolecular structures and Ca^{2+} binding. *Food Hydrocolloids*, *23*, 1746–1755.

Gaharwar, A. K., Dammu, S. A., Canter, J. M., Wu, C., & Schmidt, G. (2011). Highly extensible, iough, and elastomeric nanocomposite hydrogels from poly(ethylene glycol) and hydroxyapatite nanoparticles. *Biomacromolecules*, *12*, 1641–1650.

Gargiulo, V., Morando, M. A., Silipo, A., Nurisso, A., Pérez, S., Imberty, A., et al. (2010). Insights on the conformational properties of hyaluronic acid by using NMR residual dipolar couplings and MD simulations. *Glycobiology*, *20*, 1208–1216.

Giannoudis, P. V., Dinopoulos, H., & Tsiridis, E. (2005). Bone substitutes: An update. *Injury*, *36*, 20–27.

Hoffman, A. S. (2002). Hydrogels for biomedical applications. *Advanced Drug Delivery Reviews*, *43*, 3–12.

Il'ina, A. V., & Varlamov, V. P. (2004). Hydrolysis of chitosan in lactic acid. *Applied Biochemistry and Microbiology*, *40*, 300–303.

Kim, J., Kim, I. S., Cho, T. H., Lee, K. B., Hwang, S. J., Tae, G., et al. (2007). Bone regeneration using hyaluronic acid-based hydrogel with bone morphogenic protein-2 and human mesenchymal stem cells. *Biomaterials*, *28*, 1830–1837.

Kirkpatrick, L. D., & Francis, G. E. (Eds.). (2007). *Physics: A world view*. USA: Thomson Wadsworth.

Larsson, S., & Hannink, G. (2011). Injectable bone-graft substitutes: Current products, their characteristics and indications, and new developments. *Injury*, *42*, 30–34.

Lasagabaster, A., Abad, M. J., Barral, L., & Ares, A. (2006). FTIR study on the nature of water sorbed in polypropylene (PP)/ethylene alcohol vinyl (EVOH) films. *European Polymer Journal*, *42*, 3121–3132.

Lee, K. Y., & Mooney, D. J. (2011). Alginate: Properties and biomedical applications. *Progress in Polymer Science*, *37*, 106–126.

LeRoux, M. A., Guilak, F., & Setton, L. A. (1999). Compressive and shear properties of alginate gel: Effects of sodium ions and alginate concentration. *Journal of Biomedical Materials Research*, *47*, 46–53.

Lertsutthiwong, P., Rojsitthisak, P., & Nimmannit, U. (2009). Preparation of turmeric oil-loaded chitosan–alginate biopolymeric nanocapsules. *Materials Science and Engineering C-Biomimetic and Supramolecular Systems*, *29*, 856–860.

Li, X. X., Xu, A. H., Xie, H. G., Yu, W. T., Xie, W. Y., & Ma, X. J. (2010). Preparation of low molecular weight alginate by hydrogen peroxide depolymerization for tissue engineering. *Carbohydrate Polymers*, *79*, 660–664.

Liu, H., Li, H., Cheng, W., Yang, Y., Zhu, M., & Zhou, C. (2006). Novel injectable calcium phosphate/chitosan composites for bone substitute materials. *Acta Biomaterialia*, *2*, 557–565.

Lopes, M. A., Knowles, J. C., & Santos, J. D. (2000). Structural insights of glass-reinforced hydroxyapatite composites by Rietveld refinement. *Biomaterials*, *21*, 1905–1910.

Lopes, M. A., Knowles, J. C., Santos, J. D., Monteiro, F. J., & Olsen, I. (1999). Direct and indirect effects of P_2O_5 glass reinforced-hydroxyapatite composites on the growth and function of osteoblast-like cells. *Biomaterials*, *21*, 1165–1172.

Manojlovic, V., Djonlagic, J., Obradovic, B., Nedovic, V., & Bugarski, B. (2006). Investigations of cell immobilization in alginate: Rheological and electrostatic extrusion studies. *Journal of Chemical Technology and Biotechnology*, *81*, 505–510.

Mason, T. G., Dhople, A., & Wirtz, D. (1998). Linear viscoelastic moduli of concentrated DNA solutions. *Macromolecules*, *31*, 3600–3603.

Matrajt, G., Borg, J., Raynal, P. I., Djouadi, Z., d'Hendecourt, L., Flynn, G., et al. (2003). FTIR and Raman analyses of the Tagish Lake meteorite: Relationship with the aliphatic hydrocarbons observed in the diffuse interstellar medium. *Astronomy and Astrophysics*, *416*, 983–990.

Moore, W. R., Graves, S. E., & Bain, G. I. (2001). Synthetic bone graft substitutes. *ANZ Journal of Surgery*, *71*, 354–361.

Murakamia, T., Sawaea, Y., Horimotob, M., & Nodac, M. (1999). Role of surface layers of natural and artificial cartilage in thin film lubrication. *Tribology Series*, *36*, 737–747.

Nair, L. S., & Laurencin, C. T. (2007). Biodegradable polymers as biomaterials. *Progress in Polymer Science*, *32*, 762–798.

Nunamaker, E. A., Purcell, E. K., & Kipke, D. R. (2007). In vivo stability and biocompatibility of implanted calcium alginate disks. *Journal of Biomedical Materials Research Part A*, *83A*, 1128–1137.

Oerther, S., Maurin, A., Payan, E., Hubert, P., Lapicque, F., Presle, N., et al. (2000). High interaction alginate–hyaluronate associations by hyaluronate deacetylation for the preparation of efficient biomaterials. *Biopolymers*, *54*, 273–281.

Oliveira, S. M., Almeida, I. F., Costa, P. C., Barrias, C. C., Ferreira, M. R. P., Bahia, M. F., et al. (2010). Characterization of polymeric solutions as injectable vehicles for hydroxyapatite microspheres. *AAPS PharmSciTech*, *11*, 852–858.

Papageorgiou, S. K., Kouvelos, E. P., Favvas, E. P., Sapalidis, A. A., Romanos, G. E., & Katsaros, F. K. (2010). Metal–carboxylate interactions in metal–alginate complexes studied with FTIR spectroscopy. *Carbohydrate Research*, *345*, 469–473.

Partal, P., & Franco, J. M. (Eds.). (2007). *Rheology, Chapter: Non-Newtonian fluids*. Spain: Encyclopedia of Life Support Systems (EOLSS).

Pasparakis, G., & Bouropoulos, N. (2006). Swelling studies and in vitro release of verapamil from calcium alginate and calcium alginate–chitosan beads. *International Journal of Pharmaceutics*, *323*, 34–42.

Pawar, S. N., & Edgar, K. J. (2012). Alginate derivatization: A review of chemistry, properties and applications. *Biomaterials*, *33*, 3279–3305.

Pelletier, S., Hubert, P., Payan, E., Marchal, P., Choplin, L., & Dellacherie, E. (2000). Amphiphilic derivatives of sodium alginate and hyaluronate for cartilage repair: Rheological properties. *Journal of Biomedical Materials Research*, *54*, 102–108.

Salih, V., Georgiou, G., Knowles, J. C., & Olsen, I. (2001). Glass reinforced hydroxyapatite for hard tissue surgery. Part II. In vitro evaluation of bone cell growth and function. *Biomaterials*, *22*, 2817–2824.

Singh, J., Dutta, P. K., Dutta, J., Hunt, A. J., Macquarrie, D. J., & Clark, J. H. (2009). Preparation and properties of highly soluble chitosan–L-glutamic acid aerogel derivative. *Carbohydrate Polymers*, *76*, 188–195.

Slaughter, B. V., Khurshid, S. S., Fisher, O. Z., Khademhosseini, A., & Peppas, N. A. (2009). Hydrogels in regenerative medicine. *Advanced Materials*, *21*, 3307–3329.

Sriamornsak, P., Thirawong, N., & Korkerd, K. (2007). Swelling, erosion and release behavior of alginate-based matrix tablets. *European Journal of Pharmaceutics and Biopharmaceutics*, *66*, 435–450.

Stevens, M. M., Qanadilo, H. F., Langer, R., & Prasad Shastri, V. P. (2004). A rapid-curing alginate gel system: Utility in periosteum-derived cartilage tissue engineering. *Biomaterials*, *25*, 887–894.

Tadros, T. F. (Ed.). (2010). *Rheology of dispersions-principles and applications*. Singapore: Wiley-VCH.

Ueng, S. W., Yuan, L., Lee, N., Lin, S., Chan, E., & Weng, J. (2004). In vivo study of biodegradable alginate antibiotic beads in rabbits. *Journal of Orthopaedic Research*, *22*, 592–599.

Ulery, B. D., Nair, L. S., & Laurencin, C. T. (2011). Biomedical applications of biodegradable polymers. *Journal of Polymer Science Part B: Polymer Physics*, *49*, 832–864.

Vaccaro, A. R. (2002). The role of the osteoconductive scaffold in synthetic bone graft. *Orthopedics*, *25*, 571–578.

Vallée, F., Müller, C., Durand, A., Schimchowitsch, S., Dellacherie, E., Kelche, C., et al. (2009). Synthesis and rheological properties of hydrogels based on amphiphilic alginate-amide derivatives. *Carbohydrate Research*, *344*, 223–228.

Viswanath, D. S., Ghosh, T. K., Prasad, D. H. L., Dutt, N. V. K., & Rani, K. Y. (Eds.). (2007). *Viscosity of liquids: Theory, estimation, experiment, and data*. Netherlands: Springer.

Yucel, T., Cebe, P., & Kaplan, D. L. (2009). Vortex-induced injectable silk fibroin hydrogels. *Biophysical Journal*, *97*, 2044–2050.

Zimmermann, G., & Moghaddam, A. (2011). Allograft bone matrix versus synthetic bone graft substitutes. *Injury*, *42*, 16–21.